Lamb Wave Devices Based On Capacitive Micromachined Ultrasonic Transducers

Mohammed H. Badi, Goksen G. Yaralioglu, A. Sanlı Ergun, Sean T. Hansen, and B.T. Khuri-Yakub

Ginzton Laboratory, Stanford University, Stanford, CA 94305-4088

Abstract— **This paper describes the theory, design, and realization of a new type of Ultrasonic Lamb Wave Transducer. The excitation mechanims of this device is unlike any other as it relies on the Capacitive Micromachined Ultrasonic Transducer (CMUT). Built using fundamental integrated circuit techniques, this device has an insertion loss of 20 dB at an operating frequency of 2.1 MHz. The dominant propagating mode in the device is that of the lowest order antisymmetric flexural wave (A_0). The substrate upon which the device rests is 18 μm thick and is almost entirely made up of crystalline silicon. When configured as a delay line oscillator, the transducer functions well as a sensor to changes in environmental conditions.**

I. Introduction

Sir Horace Lamb published the first detailed treatise on Lamb waves in 1917 [1] with two goals in mind. The first goal was to better understand vibrations in a solid bounded by parallel planes with dimensions much smaller than the wavelength. The second goal was to help answer questions put forth in seismology relating to waves and vibrations in an elastic medium. Since then the characteristics of Lamb waves have been explored by many authors [2], [3] and numerous acoustic wave devices have been built using the excitation of Lamb waves as the primary vehicle of transduction. Most of these devices rely on an interdigital electrode configuration [4] and use either the piezoelectric or electrostrictive effect [5], [6]. The devices described in this paper excite and sense Lamb waves in the silicon substrate by coupling energy to and from the vibrating membrane of a Capacitive Micromachined Ultrasonic Transducer (CMUT). A proof of principle of this device, along with preliminary experimental and theoretical data, can be found in [7] - [9]. A detailed review of the current state of this technology is given in [10].

This paper begins with some background on Lamb waves and Lamb wave excitation using CMUTs. It continues with a discussion of the transducer's equivalent circuit model with an emphasis on the impedance presented to the membrane by the device substrate. After a brief description of the manufacturing process, experimental verification of the model and preliminary results of the device when used as a humidity sensor are presented. The paper concludes with a description of plans for future work.

II. Lamb Waves Using CMUTs

Lamb and Love waves describe two types of normal modes, also called plate modes, that can exist in a plate with free boundaries. In a Lamb wave the displacement of the particles occurs both in the direction of wave propagation and perpendicular to the plane of the plate. This wave has two groups of modes that can independently satisfy the wave equation: symmetric and antisymmetric [1].

The Lamb wave devices described in this paper use rectangular CMUTs as their primary vehicle of transduction. As shown in Fig. 1, the membranes are 77 μm wide, 1 cm long, and 1 μm thick with a gap of 1 μm. An aluminum electrode covers half of the surface of the membrane and acts as one of the capacitor's electrodes. The other electrode, not shown on the figure, is a thin highly doped region on the top of the silicon surface. When an AC voltage is superimposed on a DC bias and applied between the two electrodes, the membrane will vibrate with a resonant characteristic determined by the geometry of the structure. As explained in the next section, energy from this vibration then couples through the posts shown in Fig. 1 to excite Lamb waves in the silicon plate. While both of the zero-order modes are excited in the substrate, the dominant mode that propagates is the lowest-order antisymmetric flexural wave (A_0). In order to reinforce the acoustic energy created by a single CMUT, fifteen transmitting membranes are spaced with a period of one wavelength on the same substrate to foster constructive interference. Due to the large aspect ratio of the membranes, the wave propagation can be approximated as a plane wave away from the membrane in the lateral direction. The Lamb waves are sensed further down the substrate by an identical set of fifteen receiving membranes. In the case of the devices presented here, the distance between the transmitting and receiving membranes is approximately 7.8 mm.

III. Equivalent Circuit Model

Most devices fabricated using CMUT technology have membranes that closely approximate circles. Theoreti-

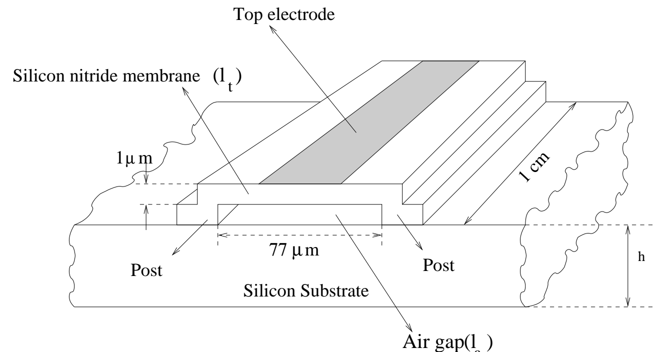

Fig. 1. Diagram of a single CMUT membrane.

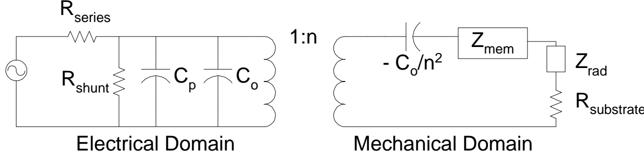

Fig. 2. Equivalent circuit model of a transmitting CMUT.

cal models for these membranes are relatively well developed [12], [13], and they have been applied to equivalent circuits that match well with experimental results [14], [15]. The membranes in the devices described in this paper, however, are rectangular, and as a result a different set of equations is necessary to describe their behavior. The derivation and presentation of these equations, for the purpose of creating an equivalent circuit model of a Lamb wave device based on CMUTs, is the subject of this section. The skeleton for this model is shown in Fig. 2 and is based on the standard equivalent circuit for an electro-mechanical transducer [16]. All of the expressions that follow treat the case of a single rectangular membrane. For a more detailed derivation of the equations associated with the model, see [10].

In Fig. 2, the parasitic C_p refers primarily to the effects of the traces on the Lamb wave device that lead from the bond pads to the membranes. In devices described in this paper, C_p is typically 20 % of the total CMUT capacitance. The parasitics R_{series} and R_{shunt} model lead resistances and membrane conductances in the transducer, respectively. The expression for R_{rad}, the radiation impedance of air, is a function of both the device aspect ratio and operating frequency and can be found in [17]. Furthermore, an expression for the electromechanical conversion factor n is derived in [15].

Expressions for C_0 and Z_{mem} are derived from the fourth order differential equation governing the normal displacement $u(x)$ of a stretched membrane under the effects of both bending stiffness and tension [12], [18]:

$$\frac{(Y_0 + T)l_t^3}{12(1-\sigma^2)}\nabla^4 u(x) - Tl_t\nabla^2 u(x) - P + l_t\rho\frac{d^2\omega}{dt^2} = 0 \,. \quad (1)$$

The variables in this equation are Young's Modulus Y_0, Poisson's Ratio σ, tensile stress T, applied pressure of P, density ρ, and angular frequency ω. The capacitance, C_0, is obtained by integrating over the resulting profile $(u(x))$. The membrane impedance, Z_{mem}, is found by converting the resulting displacement to a velocity and relating it to the applied force on the membrane.

The substrate impedance presented to the membrane, $R_{substrate}$, is found using finite element analysis[1] (FEA) and the subsequent application of normal mode theory to the results. Note that since the "current" in the mechanical part of the circuit in Fig. 2 is the membrane velocity, it is important that the definition of $R_{substrate}$ be consistent with this convention. To that end, if P_n is the average propagating power of the nth Lamb wave mode and v is the velocity of the membrane, the expression in (2) can be written for $R_{substrate}$. The assumption in this formulation is that all of the energy coupled to the substrate is in the form of a propagating mode; for this reason the right hand side of (2) is purely real. A detailed description on the calculation of the power and the velocity in this equation is given in [9], [10].

$$R_{substrate_n} = \frac{2P_n}{|\overline{v}|^2} \quad (2)$$

A plot of the impedance presented to the membrane by various thicknesses is shown in Fig. 3. Note that the there is an increased coupling of energy from the membrane to the the Lamb wave for smaller substrates.

Inherent to the definition presented in (2) for $R_{substrate}$ is the fact that the vibrating membrane is the source of

[1]Finite element calculations were performed using Ansys 5.7.

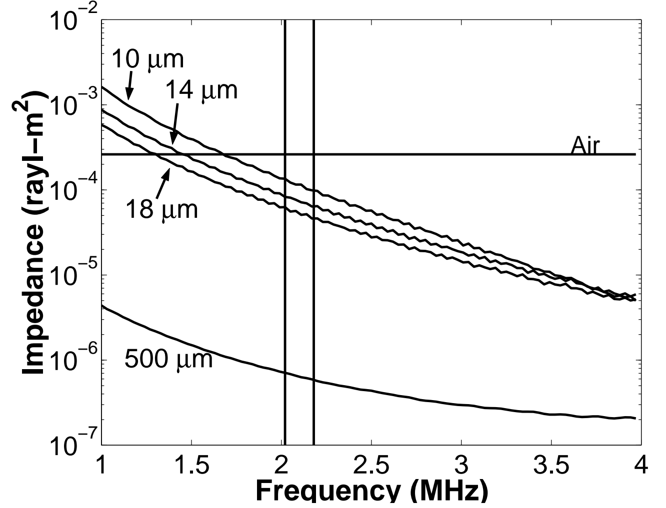

Fig. 3. Impedance presented to the vibrating membrane by device substrates of four different thicknesses. The vertical lines represent the operating frequency range of the four devices.

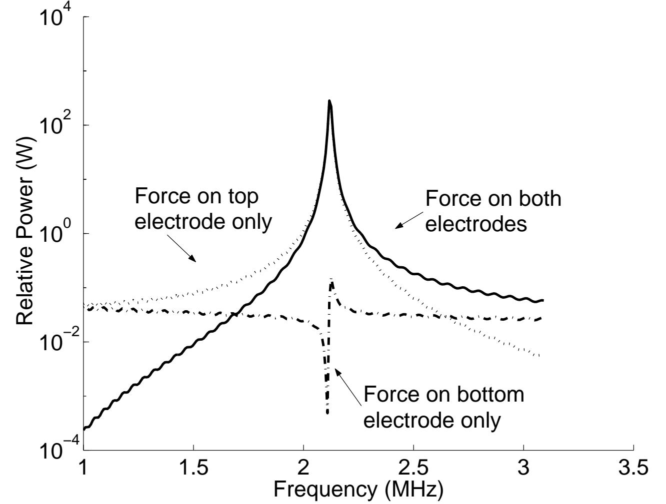

Fig. 4. Power coupled into the A_0 mode of the substrate using three different excitation mechanisms. The constants are taken from Auld: V_s = 5840.9 m/s, V_l = 8429.4 m/s, ρ = 2332 kg/m^3.

energy of the Lamb wave. The graph in Fig. 4 shows the power coupled into the A_0 mode when forces act on the device electrodes in three different configurations. In the first configuration, where the forces are on both the top and bottom electrodes, the curve shows a resonant behavior with maximum power delivered to the substrate at the resonant frequency of the membrane. In the second configuration, where the forces act on the top membrane only, almost the same amount of power is transferred to the substrate at frequencies at and around the membrane resonance. In contrast to these two cases, the energy coupled into the Lamb wave is at least three orders of magnitude smaller when the force is applied to only the bottom electrode. This graph thus clearly shows that the source of most of the energy in the Lamb wave is indeed the vibrating membrane, and that the energy is coupled through the supporting posts into the substrate. Note that 95 % of the energy coupled into the Lamb wave is in the A_0 mode. For this reason the curves for the S_0 case are not included in Fig. 4.

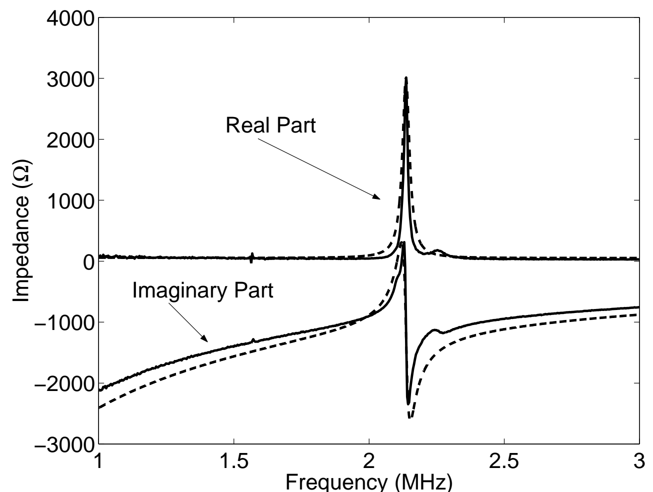

Fig. 5. Experimental (solid line) and simulated (dashed line) input impedance plots of a Lamb wave device with 15 rectangular membranes in parallel with each other on a 350 μm substrate.

IV. Device Fabrication

The process used to fabricate these Lamb wave devices is based on that of the conventional CMUT [15], [19] and is very similar to the one described in [7]. The difference comes in once the fabrication of the transducers is complete. At this point the CMUTs are characterized to determine their resonant frequency. This frequency, along with the separation of the membranes, is what determines the final substrate thickness of the device. In the specific case of the transducers presented here, the substrate was thinned down to 18 μm. This thinning procedure can be performed using a wet etchant such as KOH or tetramethyl ammonium hydroxide (TMAH). The former option capitalizes on the perfect masking ability of silicon nitride in KOH [20] and was therefore chosen for use in this process. Due to the high etch rate of aluminum in KOH, a fixture was used to shield the device side of the wafer from the etchant. This fixture, similar to others found in the literature [21], [22] is comprised of two halves of peek that come together over a wafer using a friction o-ring seal. Since the final substrate thickness could not be determined until after the membranes had been built and their resonances had been measured, an etch stop could not be incorporated into the wafer.

V. Experimental Results and Discussion

The model described by Fig. 2, along with its supporting equations, is verified by experiment (see Fig. 5). This figure presents simulated and experimental input impedance plots for fifteen rectangular membranes in parallel with each other. Both the overall shape of the curves and the relative values are similar to what is normally seen in the case of a circular CMUT. Furthermore, the measured resonant frequency and input impedance values agree well with theory, while the bandwidth of the transducer is smaller than predicted by the equivalent circuit. This discrepancy is most likely due to the approximations used in the radiation and device impedance models. Note that in order to satisfy the assumption in the discussion of Fig. 2 that $R_{substrate}$ is small, the transducers used in this measurement have a substrate thickness of 350 μm.

As shown in Fig. 6, the device has an insertion loss of 20 dB at frequencies near the maximum membrane displacement, 2.1 MHz, once its substrate is thinned down to 18 μm. This value is attained despite a mismatch between the optimum thickness of the silicon plate (determined by the separation of the CMUT membranes to be 22 μm) and its actual value of 18 μm. The result of the mismatch is destructive interference of the Lamb waves in the silicon substrate.

When Lamb wave devices are used as sensors they are often wired up as delay-line oscillators and are sensitive to mass loading of the substrate [5], [10]. One way to change the mass loading is to vary the humidity in the environ-

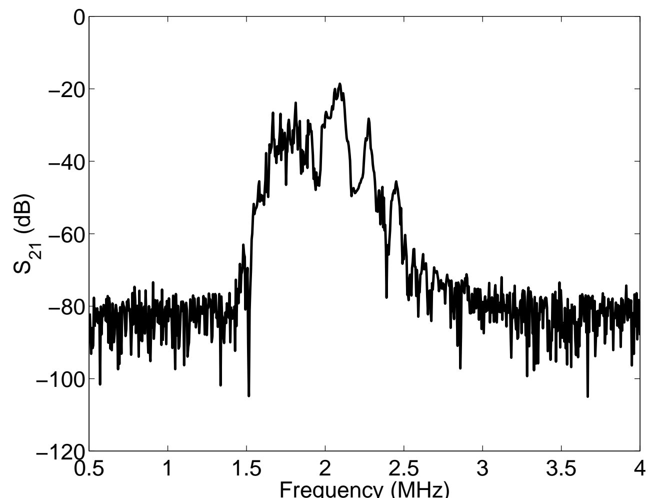

Fig. 6. An S_{21} measurement of a Lamb wave device. Note that the insertion loss near 2.1 MHz is 20 dB.

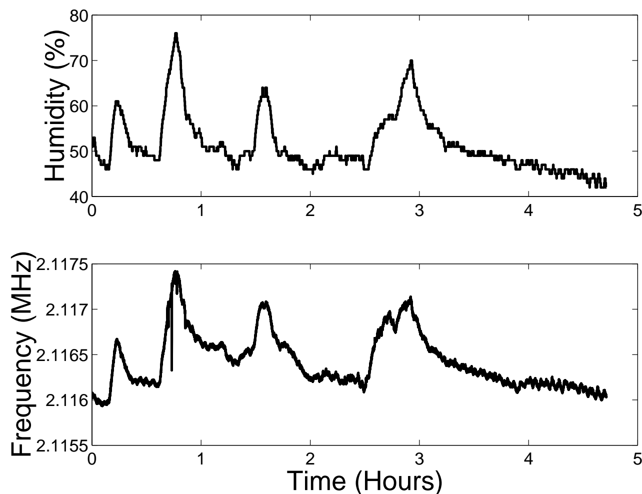

Fig. 7. Humidity measurement at 23 ^{o}C.

ment of the device to cause either absorption or desorption of moisture by the material in the channel. Figure 7 shows the results of an experiment in which the relative humidity around the Lamb wave device changed as a function of time and the temperature was held constant at 23 ^{o}C. The top graph shows data taken from an off-the-shelf humidity sensor (Omega-RH411) while the bottom graph shows the frequency of the oscillator. The two curves have a similar shape although the response of the oscillator is slower than that of the humidity sensor. This behavior is expected because the top of the device channel is composed of silicon nitride which is a hydrophilic material that does not easily desorb moisture. The humidity sensor, on the other hand, is designed to respond quickly to moisture changes in its environment. When evaluating Fig. 7 it is important to remember that the purpose of this experiment was not to show that the Lamb wave device could work as an ideal humidity sensor, but rather that it could respond as one would expect to mass loading.

One additional comment that should be made regarding this experiment is that the CMUT membranes are also affected by changes in the humidity . This phenomenon has little effect on the resulting behavior of the device, however, as the resonant frequency of a vibrating membrane decreases in the presence of mass loading. Since this is the opposite direction of what is measured in Fig. 7, the humidity effects on the channel are dominant in the results presented here.

VI. Conclusion

Using Capacitive Micromachined Ultrasonic Transducers (CMUTs), an efficient Lamb wave device has been built. This paper has described these devices by touching on their theory, fabrication, and characterization. The proposed equivalent circuit model and accompanying equations that were presented predict an input impedance that matches well with what is observed by experiment. The insertion loss of the transducer is 20 dB. The device functions well as a sensor in response to changes of the mass loading of its channel caused by a variation in the humidity in its environment. Future work on these Lamb wave devices includes the fabrication of transducers with a larger substrate resistance as well as a more detailed analysis of the device behavior as a sensor and its response to different measurands.

References

[1] H. Lamb, *Proc. Roy. Soc. (London), Ser. A*, Vol 93, p. 114, 1917.

[2] I.A. Viktorov, *Rayleigh and Lamb Waves*, Plenum: New York,NY 1967.

[3] B.A. Auld, *Acoustic Fields and Waves in Solids*, 2d Ed., Krieger: Malabar, FL, 1990

[4] R.M. White, "Surface Elastic Waves," *Proc. IEEE*, Vol. 58, No. 8, pp. 1238-76, 1970.

[5] S.W. Wenzel, *Applications of Ultrasonic Lamb Waves*, Doctoral Dissertation, EECS Department, University of California, Berkeley, CA, 1982.

[6] S.W. Wenzel and R.M. White, "A Multisensor Employing and Ultrasonic Lamb Wave Oscillator", *IEEE Trans. Electron Devices*, Vol. 35, pp. 735, 1988.

[7] M. H. Badi, G. G. Yaralioglu, A. S. Ergun, F. L. Degertekin, C. H. Cheng, B. T. Khuri-Yakub, "A First Experimental Verification of Micromachined Capacitive Lamb Wave Transducers," in *Proc. IEEE Ultrasonics Symposium*, Vol. 1, pp. 311-314, 2000.

[8] G.G. Yaralioglu, M.H. Badi, A.S. Ergun, C.H. Cheng, F.L. Degertekin, B.T. Khuri-Yakub, "Lamb Wave Devices Using Capacitive Micromachined Ultrasonic Transducers," *Applied Physics Letters*, Vol. 78, pp. 111-113, 2001.

[9] G.G. Yaralioglu, F.L. Degertekin, M.H. Badi, B.A. Auld, and B.T. Khuri-Yakub, "Finite Element Method and Normal Mode Modeling of Capacitive Micromachined SAW and Lamb Wave Transducers," *2000 Ultrasonics Symposium Proceedings*, pp. 129-132, 2000.

[10] M.H. Badi, G.G. Yaralioglu, A.S. Ergun, S.T. Hansen, E.J. Wong, and B.T. Khuri-Yakub, "Capactive Mircomachined Ultrasonic Lamb Wave Transducers," submitted to *IEEE Trans. Ultrason. Ferroelect. Freq. Contr.*, 2002.

[11] R.M. White, P.J. Wicher, S.W. Wenzel, and E.T. Zellers, "Plate-mode Ultrasonic Sensors," *IEEE Trans. Ultrasonics, Ferroelectrics, Frequency Control*, Vol. 34, No. 2, pp. 162-171, 1987.

[12] W.P. Mason, *Electromechanical Transducers and Wave Filters*, New York: D. Van Norstrand Co., Inc., 1942.

[13] L.L. Beranek, *Acoustics*, Woodbury: Acoustical Society of America, 1996.

[14] A. Caronti, G. Caliano, A. Iula, and M. Pappalardo, "An Accurate Model For Capacitive Micromachined Ultrasonic Transducers," *IEEE Trans. Ultrasonics, Ferroelectrics, Frequency Control*, Vol. 49, No. 2, pp. 159-168, 2002.

[15] X. Jin, "Micromachined Capacitive Ultrasonic Immersion Transducer Array," Doctoral Dissertation, Electrical Engineering Department, Stanford University, Stanford, CA, 2000.

[16] F.V. Hunt, *Electroacoustics*, Acoustical Socity of America, 1982.

[17] P.R. Stepanishen, "The Radiation Impedance of a Rectangular Piston," *J. Sound and Vibration*, Vol. 55, pp. 275-288, 1977.

[18] J.W. (Lord Rayleigh) Strutt, *The Theory of Sound Vol. 1*, New York: Macmillan, 1877-78.

[19] V. Foglietti, D. Memmi, G. Caliano, E. Cianci, F. Galanello, M. Pappalardo, "Fabrication of Micromechanical Capacitive Ultrasonic Transducers By Surface Micromachining," in *Proceedings of the International Conference on Microtechnologies*, Vol. 1, pp. 79-82, 2000.

[20] H. Seidel, L. Csepregi, A. Heuberger, H. Baumg'artel, "Anisotropic Etching of Crystalline Silicon in Alkaline Solutions," *J. Electrochem. Soc*, Vol. 13, No. 11, pp. 3612-25, 1990.

[21] C-H. Han, E.S. Kim, "Fabrication of Dome-Shaped Diaphragm With Circular Clamped Boundary On Silicon Substrate," *12th Intl. Workshop on Micro Electro Mechanical Systems*, pp. 505-510, 1999.

[22] G.C. Hilton, J.M. Martinis, K.D. Irwin, N.F. Bergren, D.A. Wollman, M.E. Huber, S. Deiker, S.W. Nam, "Microfabricated Transisiton-Edge X-Ray Detectors," *IEEE Transactions on Applied Superconductivity*, Vol. 11, No. 1, Pt. 1, pp. 739-742, 2001.